Controlled Positioning of Carbon Nanotubes by Dielectrophoresis: Insights into the Solvent and Substrate Role

Martial Duchamp,[†] Kyumin Lee,[†] Benjamin Dwir,[‡] Jin Won Seo,[§] Eli Kapon,[‡] László Forró,[†] and Arnaud Magrez[†,⊥,*]

[†]Laboratoire de Nanostructures et Nouveaux Matériaux Electroniques (LNNME), Ecole Polytechnique Fédérale de Lausanne (EPFL), CH-1015 Lausanne, Switzerland, [‡]Laboratory of Physics of Nanostructures (LPN), Ecole Polytechnique Fédérale de Lausanne (EPFL), CH-1015 Lausanne, Switzerland, [§]Department Metallurgy and Materials Engineering, Katholieke Universiteit Leuven, B-3001 Heverlee, Belgium, and [⊥]Center for Research on Electronically Advanced Materials, Ecole Polytechnique Fédérale de Lausanne (EPFL), CH-1015 Lausanne, Switzerland

ABSTRACT We demonstrate the ability to precisely control the deposition of a defined number of carbon nanotubes (CNTs) from solution onto microfabricated electrodes using dielectrophoresis. The solvation shell around the CNTs, exhibiting a high dielectric constant which is possibly larger than the intrinsic dielectric constant of CNTs, is found to play a crucial role in electrophoretic processes. Substrate resistivity is also very important: The spatial repartition of the electric field between the substrate and the microelectrodes leads to deviations from the precise location of the CNTs. A recipe is given for the dielectrophoresis of CNTs which can be extended to other nanowires or nanotubes.

Controlled positioning is one of the most significant hurdles in the application of carbon nanotubes (CNTs).[1−4] Chemical vapor deposition (CVD), involving the decomposition of a carbon source over a catalyst particle, overcomes this drawback by *a priori* control of the nanotube growth site, when catalyst positioning is possible on the device structure.[5] However, devices rarely tolerate the typical CVD growth temperatures, and the synthesis of high quality CVD CNTs at low temperature remains a subject of intensive research. Although significant progresses have been achieved in the optimization of the CVD process in terms of product quality,[6,7] catalytically grown CNTs still exhibit high density of structural defects,[8] which make them inappropriate for several applications, in particular those involving individual CNTs. In contrast, arc discharge (AD) sublimation or laser ablation of graphite allows high quality CNT synthesis[9] with defect-free structures. AD-grown CNTs often exhibit exceptional properties, close to the ones predicted by theory.[10] Therefore, they are of particular interest for the construction of device prototypes despite the fact that only a small quantity is available. Nevertheless, CNT handling is difficult as AD-synthesis methods do not allow growing CNTs directly on a device. Moreover, AD-grown CNTs require several subsequent purification and dispersion steps resulting in a CNTs suspension. Therefore, the biggest challenge is to controllably deposit individual CNTs on substrates out of colloidal solutions of AD-grown CNTs at specific device locations.

Different methods exist to deposit CNTs on a surface; the most intuitive approach is to place a drop of suspension and wait for the solvent evaporation. This method has recently been improved by the so-called "boil deposition"[11] which avoids agglomeration by boiling the solvent during the drying step. A second method consists of surface modification combined with dip coating which allows positioning and orientation of CNT arrays.[12] Unfortunately, both methods do not provide the possibility to precisely position individual CNTs. Nanomanipulation using a scanning probe microscope makes the precise placement and the realization of individual nanodevices possible;[13] however, this low-scale and highly time-consuming process does not afford wafer-range applications. A promising technique for mass-scale assembly of individual CNTs is the microelectrode dielectrophoresis (DEP) which allows controlling deposition of CNTs from colloidal solutions.[14] DEP deposition yields CNTs in contact with electrodes which makes the method particularly suitable for the application of CNTs as electronic devices.

Described simply, a drop of CNT solution is applied over a pair of opposing

*Address correspondence to arnaud.magrez@epfl.ch.

Received for review November 4, 2009 and accepted December 21, 2009.

Published online January 7, 2010.
10.1021/nn901559q

microelectrodes between which an AC voltage is applied, attracting CNTs to the electrode boundaries, where they stay after the solvent dries up. Depending on the electrode geometry and the nanotube length, a CNT may bridge the electrode pair. Previous works have studied the effects of CNT chirality,[15] AC/DC voltage level and signal frequency,[16] as well as the electrode geometry.[14] Despite these numerous studies, the role of solvent and the interaction of solvent molecules with CNTs as well as the electric coupling, which appears between the substrate and the electrodes, have been overlooked so far. In this work, we demonstrate that both the solvent and the substrate are the major players in the dielectrophoresis of CNTs. More specifically, the dielectric permittivity of the CNT solvation shell and the pattern of the electric field as dictated by the substrate resistivity lead to qualitative and quantitative differences in the DEP results. We also present the experimental parameters that lead to single-CNT bridging of electrode pairs.

Multiwalled CNTs were produced by AD. Detailed information on the production process is reported elsewhere.[17,18] CNTs are high quality materials with low defect density as detailed Raman scattering spectroscopy revealed.[18] Scanning electron micrographs of AD multiwalled CNTs (MWCNTs) revealed a tube length of 200−4000 nm (see Supporting Information, Figure S1). CNTs were dispersed in three different solvents to prepare colloidal solutions: deionized water, isopropyl alcohol (IPA), and cyclohexanone. These solvents have been frequently used in the literature in order to prepare CNTs suspensions. In 100 mL of each solvent, 0.2 mg of CNT powder was dispersed using an ultrasonic finger.[19] The proper and damage-free dispersion of individual CNTs was verified by scanning electron microscopy (SEM) study of boiled-off deposits prepared after the DEP experiments. Colloidal stability of the prepared CNT solutions was monitored through optical absorption measurements; agglomeration results in a decrease of optical absorption. All these surfactant-free solutions were stable for the time frames relevant to the DEP experiments, confirmed by high and stable optical absorption for at least 20 min after sonication (see Supporting Information, Figure S2).

Microelectrode pairs of 2 μm gaps were fabricated by photolithography and lift-off on different substrates: silicon (Si) wafers with different thicknesses of thermally grown oxide layer, quartz, glass, and GaAs. DEP was carried out on the patterned substrates, each within a few minutes after sonication. A 100 μL drop of CNT solution was deposited over 20 electrode pairs (see Supporting Information, S3), while V_{TOT} (being the sum of equal amplitude of DC (V_{DC}) and AC rms value (V_{AC}, f = 1 MHz) voltages) was applied. Using equal values of V_{DC} and V_{AC} (rms) amplitudes was found to give optimal results.[16] The drop was left for 2 minutes, and the substrates were then thoroughly dried with a stream of nitrogen gas.

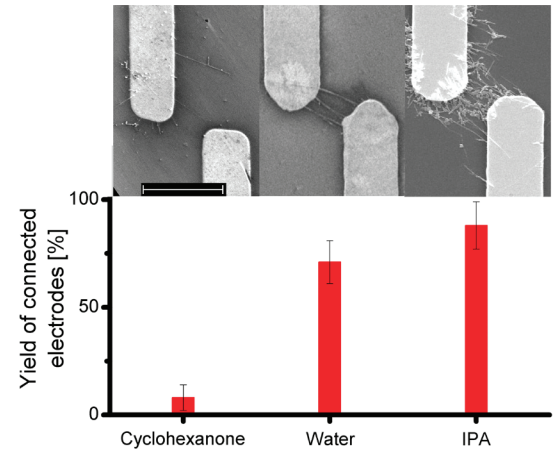

Figure 1. Statistics of electrode connection yield after dielectrophoresis of CNTs dispersed in cyclohexanone, water, and IPA solvents: 2 V_{TOT} was applied on silicon wafer with 2 μm of oxide layer. Electrode connection yield was measured over 20 electrode pairs for each solvent. Representative SEM micrographs are presented for each solvent with a scale bar of 5 μm. Error bars represent 1 SD of the measurement results.

The resulting deposits were studied by SEM. In particular, the number of connected electrodes was counted in order to determine the yield. Results of DEP carried out with different solvents are summarized in Figure 1. As the statistics show, water- and IPA-based CNT solutions reveal high probability of "success": the majority of electrode pairs are bridged by CNTs. In contrast, the cyclohexanone-based solution shows a significantly lower yield. All CNT solutions had nearly identical concentration of dispersed CNTs, as verified by optical absorption measurements and boiled-off deposit studies. Other experimental parameters such as the substrate and the applied voltage were kept constant. Consequently, the differences in yield have to be attributed solely to the solvent effect.

For CNT solutions containing low-conductivity solvent and neutral pH, the dielectrophoretic force exerted on a tube with its major axis parallel to an inhomogeneous alternating electric field is described by the following equation:

$$F_{DEP} = \frac{\pi d^2 l}{8}\varepsilon_m \mathcal{R}e\left(\frac{\varepsilon^*_{CNT} - \varepsilon^*_m}{\varepsilon^*_m + (\varepsilon^*_{CNT} - \varepsilon^*_m)L}\right)\nabla E^2 \qquad (1)$$

where ∇E is the average gradient of the electric field over the volume of the nanotube; ε^*_{CNT} and ε^*_m are the complex dielectric constant of the CNTs and of the solvent, respectively. The depolarization factor L is of the order of 10^{-4} for a CNT with a diameter of 5 nm and a length of 1 μm.[15]

A net force F appears when the dielectric constants of the nanotube and of the solvent are different. The di-

electric constants of the solvents employed here are 16.1 (cyclohexanone), 20.18 (IPA), and 78.36 (water).[20] Hence, the solvent-derived yield differences in the DEP dielectrophoretic experiments, as presented in Figure 1, cannot be explained by the DEP standard approach based on the difference between the CNT and the solvent dielectric permittivity.[21] For surfactant-free suspension, the first layers of solvent molecules ordered on the CNTs surface, the solvation shell, induce a local modification of the dielectric permittivity.

For water-based CNT solutions, calculations reveal that water molecules are aligned tangential to the CNT surface,[22] to minimize the surface and electrostatic energies.[23] However, the interaction between water and graphitic structures is generally weak: The calculated water adsorption energy on graphite surfaces is about 3 kcal/mol.[24] Therefore, the dipole moments of the solvation shell, based on freely rotating water molecules, can align along the direction of the applied electric field (Figure. 2a). This induces a dielectric permittivity of the solvation shell along the CNT axis. The maximum dipole moment of the first water molecules layer of the solvation shell is about 500kD per micrometer length of a 5 nm-diameter CNT when all water molecules are aligned along the electric field direction. On the other hand, metallic nanotubes have been predicted to have infinite permittivity, but the finite length and the presence of defects effectively lead to a finite permittivity.[25,26] The polarizability of a 1 μm length CNT is calculated to be about 530 kD for an electric field of 1 V/μm. Consequently, when all water molecules are aligned along the electric field, the dipole moment of the solvation shell is contributing to the DEP force by the same amount as does the dipole moment of the CNT itself.

The adsorption energy of IPA molecules on graphite is much higher than that of water molecules. However, the dipole moment is parallel to the O−H bond of the molecule. The sp^3 hybridization of carbon, to which the OH group is attached, allows the dipole moment to freely rotate (Figure 2b). Therefore, the dipole moment of the IPA solvation shell - considering the dipole moment of IPA,[28] and the number of adsorbed IPA molecules per unit length of CNTs[27] - is about the same order of magnitude as that of the solvation shell of water; the latter being larger than the dipole moment of the CNTs. Consequently, the dielectric permittivity of the IPA solvation shell along the CNT axis is approximately as large as that of the water solvation shell. Therefore, the DEP forces applied to the MWCNTs solvated by water or IPA are similar resulting in comparable yield of connected electrodes (Figure 1).

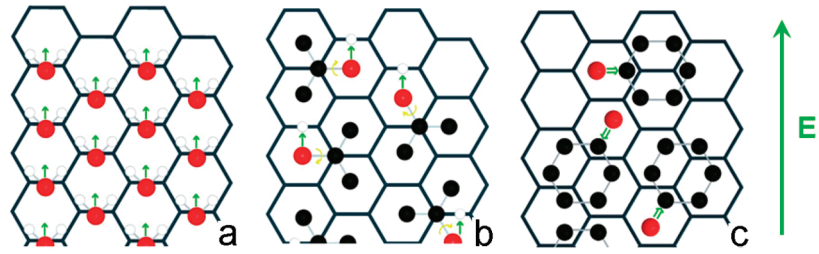

Figure 2. Arrangement of solvent molecules on a graphitic surface which is similar to CNT surface for (a) water, (b) IPA, and (c) cyclohexanone when an electric field *E* is applied. The hydrogen atoms bonded to the carbon atoms are not shown; black, red, and white balls represent carbon, oxygen, and hydrogen atoms, respectively. The small green arrows represent the direction of the dipole moment aligned in the electric field direction for water and IPA and the respective alignment of the molecule for cyclohexanone. The number of molecules per carbon cycles corresponds to calculated value from ref 24 for water and ref 27 for IPA and cyclohexanone.

For cyclohexanone, the adsorption energy on CNTs is as high as for IPA.[27] Nevertheless, the dipole moment of the cyclohexanone molecule is pointing along the carbonyl (C═O) group. The ketone molecule being cyclic and the C of the carbonyl group being sp^2 hybridized, the dipole moment of cyclohexanone molecules adsorbed on CNTs cannot freely rotate and therefore cannot align along the dielectric field (Figure 2c). Therefore, the dielectric permittivity of the cyclohexanone solvation shell cannot significantly contribute to the DEP force applied, and the yield of DEP experiments is low. Consequently, the dielectric constant of the solvation shell must be included into the force calculations, in addition to the dielectric constant of CNTs, in order to take the solvent effect correctly into account. Thus, the dielectrophoretic force thus becomes:

$$F_{DEP} = \frac{\pi d^2 l}{8}\varepsilon_m \mathcal{R}e\left(\frac{\varepsilon^*_{CNT+SS} - \varepsilon^*_m}{\varepsilon^*_m + (\varepsilon^*_{CNT+SS} - \varepsilon^*_m)L}\right)\nabla E^2 \quad (2)$$

where (ε^*_{SS+CNT}) is the complex dielectric constant of the solvated CNTs.

For the present work, pristine nanotubes dispersed in solvents have been studied. However, chemically modified, functionalized CNTs (with polarizable functional groups) are expected to significantly affect the polarizability of CNTs and, consequently, the dielectrophoresis yield. This will be the subject of future studies.

In the microelectrode DEP of CNTs, the goal is often to have a defined number of CNTs bridging the electrode gap (one or more). Having uniform CNT deposits around the whole electrode is not desirable. The degree of deposits can be quantified with the "bridge-to-deposit ratio", which describes the ratio between the substrate area between an electrode pair (green ellipses in Figure 3) and the total substrate area covered by CNT deposits. This bridge-to-deposit ratio is 1 when all deposited CNTs bridge an electrode pair and ~0 when CNTs are deposited uniformly around the electrodes without connecting

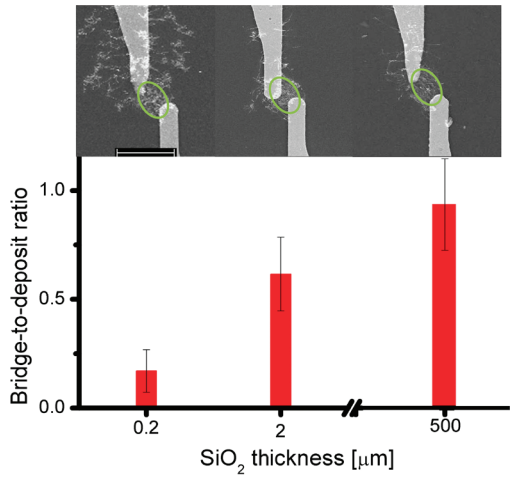

Figure 3. Bridge-to-deposit ratio (area between electrodes, green ellipses, over area covered by CNTs) around microelectrode pairs obtained for substrates covered with SiO_2 layer and for 500 μm thick quartz substrate. Ratios were measured over 20 electrode pairs used for dielectrophoresis from CNTs suspended in IPA. Representative SEM micrographs are presented for each solvent. Scale bar is 10 μm. Error bars represent 1 SD of the measurement results.

the electrodes. We found that the dielectric layer thickness and substrate resistivity are important factors for the resulting deposit pattern. On Si substrates with a thin oxide layer of 200 nm, the undesirable pattern with uniform-deposit was observed, whereas Si substrates with a thick oxide layer of 2 μm resulted in a pattern with high degree of bridging-deposits. The best results were obtained for 500 μm thick quartz substrates (Figure 3). Ideal bridging deposits were also obtained with GaAs and glass substrates.

The effect of the substrate on the bridge-to-deposit ratio can be explained by calculating the pattern of the electric field around the microelectrode pairs (Figure 4). Finite element simulations were performed on the basis of (i) 50 nm thick gold electrodes deposited on top of 200 nm SiO_2 supported by a silicon substrate (10 S/m) (see Figure 4a,b) and (ii) a quartz substrate (500 μm thick, 10^{-14} S/m) (see Figure 4d,e). In Figure 4 panels a and d, the electrodes are separated by a 1 μm wide gap (marked by A−A′ in the SEM image), and the electrodes in Figure 4 panels b and e represent the side of a single electrode (marked by B−B′ in the SEM image). The silicon substrate and one electrode of the microelectrode pair are fixed at the electric ground level (the silicon substrate is grounded through the sample holder, and the electrode is grounded through the function generator). Even if an insulating layer exists between the electrodes and the substrate, the electric field shape still induces uniform deposits around the ungrounded electrode if the oxide is too thin (Figure 4c). The DEP force at the electrode sides (Figure 4b) is found to be as high as between two electrodes for 200 nm of SiO_2 layer (Figure 4a) on top of the 10 S/m silicon substrate. In contrast, the DEP force is found to be almost negligible at the electrode sides when an insulating quartz substrate is used (Figure 4e) leading to preferential CNT placement between the two electrodes (Figure 2 and Figure 4f).

Controlled positioning of CNTs by the DEP method was found to be substrate independent when insulating substrates are used. Results obtained with insulating polymers like nylon, Teflon, PMMA, and PVC are

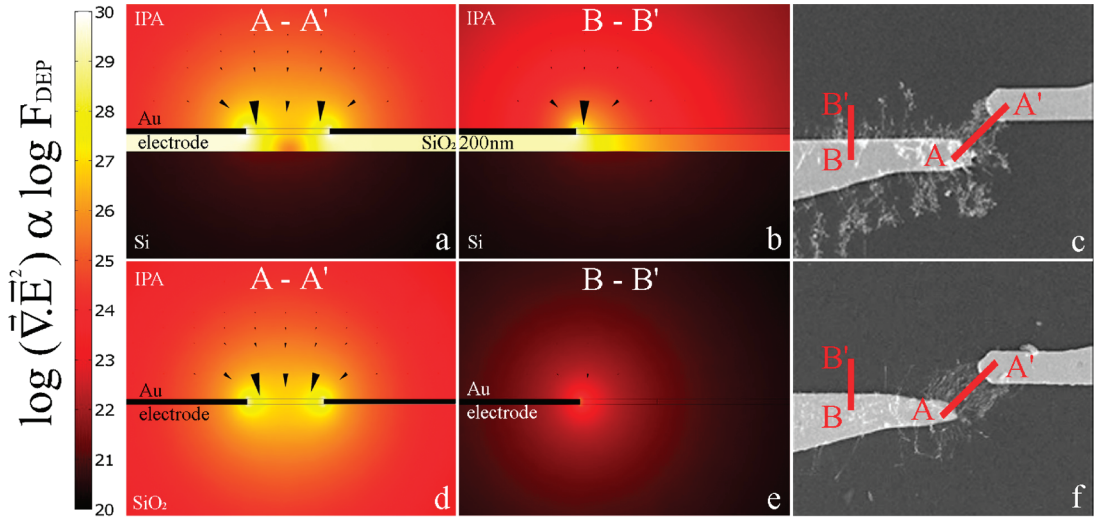

Figure 4. Finite element simulation of the gradient of the squared electric field, proportional to the DEP force, around gold metallic electrodes (black squares) on top of a silicon wafer (10 S/m) coated with a 200 nm SiO_2 layer (a,b) or on 500 μm thick quartz (d,e). The simulations correspond to cross sections taken at the points (A−A′ and B−B′) denoted by red lines in the SEM micrographs (c,f) of CNTs attracted around the microelectrodes (top view) on the corresponding substrates. The colors and the arrows represent the magnitude (in log scale) and the direction of the gradient of the squared electric field, respectively. The electric field propagation into the insulating substrate, below the gold electrodes (d), is shown to enhance the SiO_2 layer effect.

similar to the ones obtained on quartz, so that devices could be fabricated in the future on flexible organic substrates by means of the DEP process. Moreover, DEP of CNTs can be achieved on highly conducting substrates like doped Si or metals as long as a thick insulating layer is intercalated between the electrodes and the substrate. As we see in the Figure 5, substrates whose conductance is smaller than 10^{-2} S/m do not need an additional insulating layer. On the other hand, substrates with conductance above 1 S/m need an oxide layer thicker than 2 μm (twice the gap between the electrodes), preferably 20 μm, to show high selectivity of CNT placement. We notice that the electrical field gradient between the nongrounded electrode and the substrate is dramatically reduced (yielding an electric field shape that induces bridging deposits) when a SiO_2 layer as thin as 2 nm, typically used in the current silicon technology, is employed on top of 1 S/m Si. In the intermediate conductivity range (between 10^{-2} and 1 S/m), the insulating layer thickness required for a controlled positioning of CNTs between the electrodes strongly depends on the thickness of the dielectric (see Supporting Information, S3)

After studying the solvent and substrate effects in the DEP of CNTs, we now address the experimental parameters that lead to single-CNT bridging over microelectrode pairs. IPA-based CNT solution and silicon substrate with 2 μm oxide layer were used to achieve high electrode connection yield. As the DEP force depends on the square of the gradient field eq 2, the variation of V_{TOT} modifies the size of the attraction region leading to a variation of the number of attracted CNTs in a given time. By adding 1 GΩ resistance in series with the electrodes,[13] the bridging of the electrodes by CNTs reduces immediately the voltage drop across the electrodes, thus decreasing the DEP force and the deposition rate. In this way, we can control the number of attracted CNTs by choosing the applied voltage and the deposition time. Figure 6 shows the distribution of the number of attracted CNTs for three different voltage values applied. For V_{TOT} = 0.7 V, 30% of the microelectrode pairs attracted a single CNT and only 10% of the electrodes were left without CNTs, while the rest (60%) attracted two or more CNTs. For V_{TOT} = 1 V, all the microelectrodes attracted at least one CNT, but the majority (about 30%) yielded 3 CNTs.

In summary, our results demonstrate that the solvent and substrate effects are crucial parameters in the DEP of carbon nanotubes. Depending on the solvent, the dielectric constant of the solvation shell is often as important as the dielectric constant of the CNT. Solvents having a low solvation shell dielectric constant should be used when the aim of DEP is the separation of conducting CNTs. The undesirable "uniform deposits", which represent a practical problem of DEP experiments in general, were found to be caused by the deformation of the electric field

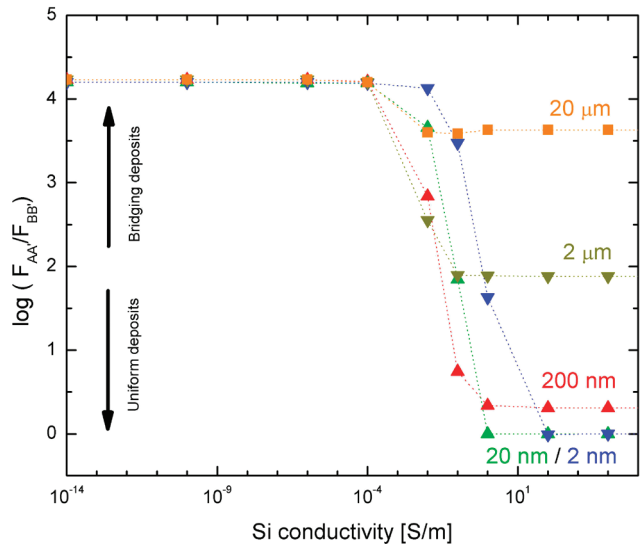

Figure 5. Ratio between the DEP force between the electrodes (indicated AA′ in Figure 3) and the lateral DEP force (indicated BB′ in Figure 4) as a function of Si substrate conductivity for various SiO_2 layer thickness on top (given in nanometers on the graph). A high ratio value indicates a DEP attraction favorable between electrodes and high degree of control of CNT localization. For the transition values of log($F_{AA'}/F_{BB'}$), the attraction between the two electrodes ($F_{AA'}$) and between the substrate and the electrode ($F_{BB'}$) are in competition. For low values of SiO_2 thicknesses, the electric field is highly confined between the electrodes and the substrate which decreases the lateral DEP force (see Supporting Information, S4).

due to the proximity of a low resistivity substrate. Good insulators such as glass or quartz are suitable as substrates for obtaining ideal "bridging deposits". Doped silicon substrates can be appropriate if an insulating layer of sufficient thickness (at least twice the interelectrode spacing) is grown on the substrate under the electrodes. The solvent and substrate effects have been exploited to obtain a reliable recipe for single-CNT bridging of microelectrodes. We also obtained comparable yields for ZnO, TiO_2, and VO_x nanowires (see Sup-

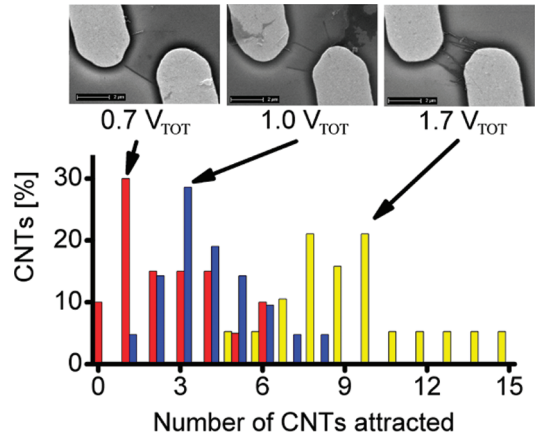

Figure 6. Distribution of the number of CNTs attracted between the microelectrode pairs as a function of applied voltages, V_{TOT}; 20 electrode pairs were measured for each voltage. Dielectrophoresis of CNTs dispersed in IPA was performed on Si wafers coated with 2 μm SiO_2: (red) V_{TOT} = 0.7 V, (blue) V_{TOT} = 1 V, (yellow) V_{TOT} = 1.7 V.

porting Information, Table S1) indicating that these results are not limited to CNTs but can be extended to other nanowires and nanotubes. Consequently, taking our observations into account, the DEP can be reliably used for the controlled placement of nano-objects on a large scale.

Acknowledgment. We thank the Centre Interdisciplinaire de Microscopie Electronique (CIME) at EPFL for access to electron microscopes and technical support and Z. Albert for the drawing of the molecule pictures. This work was financially supported by the National Centre of Competence in Research (NCCR) "Nanoscale Science" of the Swiss National Science Foundation.

Supporting Information Available: CNTs length distribution, stability of the CNTs suspensions by optical absorption, SEM micrographs of the microelectrodes, DEP parameters to attract individual nanowires/nanotubes made from various materials. This material is available free of charge *via* the Internet at http://pubs.acs.org.

REFERENCES AND NOTES

1. Ding, D.; Chen, Z.; Rajaputra, S.; Singh, V. Hydrogen Sensors Based on Aligned Carbon Nanotubes in an Anodic Aluminum Oxide Template with Palladium as a Top Electrode. *Sens. Actuators B* **2007**, *124*, 12–17.
2. Fennimore, A. M.; Yuzvinsky, T. D.; Han, W. Q.; Fuhrer, M. S.; Cumings, J.; Zettl, A. Rotational Actuators Based on Carbon Nanotubes. *Nature* **2003**, *424*, 408–410.
3. Baughman, R. H.; Cui, C.; Zakhidov, A. A.; Iqbal, Z.; Barisci, J. N.; Spinks, G. M.; Wallace, G. G.; Mazzoldi, A.; De Rossi, D.; Rinzler, A. G.; *et al*. Carbon Nanotube Actuators. *Science* **1999**, *284*, 1340–1344.
4. Hall, A. R.; Falvo, M. R.; Superfine, R.; Washburn, S. A Self-Sensing Nanomechanical Resonator Built on a Single-Walled Carbon Nanotube. *Nano Lett.* **2008**, *8*, 3746–3749.
5. Oh, B. S.; Min, Y. S.; Bae, E. J.; Kang, D. H.; Jung, I. S.; Hwang, C. S.; Kim, Y. K.; Park, W. Fabrication of Suspended Single-Walled Carbon Nanotubes *via* a Direct Lithographic Route. *J. Mater. Chem.* **2006**, *16*, 174–178.
6. Ebbesen, T. W.; Takada, T. Topological and sp^3 Defect Structures in Nanotubes. *Carbon* **1995**, *33*, 973–978.
7. Magrez, A.; Seo, J. W.; Kuznetsov, V. L.; Forró, L. Evidence of an Equimolar $C_2H_2-CO_2$ Reaction in the Synthesis of Carbon Nanotubes. *Angew. Chem., Int. Ed.* **2007**, *46*, 441–444.
8. Lee, K.; Lukic, B.; Magrez, A.; Seo, J. W.; Briggs, G. A. D.; Kulik, A. J.; Forró, L. Diameter-Dependent Elastic Modulus Supports the Metastable-Catalyst Growth of Carbon Nanotubes. *Nano Lett.* **2007**, *7*, 1598–1602.
9. Ebbesen, T. W.; Ajayan, P. M. Large-Scale Synthesis of Carbon Nanotubes. *Nature* **1992**, *358*, 220–222.
10. Treacy, M. M. J.; Ebbesen, T. W.; Gibson, J. M. Exceptionally High Young's Modulus Observed for Individual Carbon Nanotubes. *Nature* **1996**, *381*, 678–680.
11. Lee, K.; Duchamp, M.; Kulik, G.; Magrez, A.; Seo, J. W.; Jeney, S.; Kulik, A. J.; Sundaram, R. S.; Brugger, J.; Forró, L. Uniformly Dispersed Deposition of Colloidal Nanoparticles and Nanowires by Boiling. *Appl. Phys. Lett.* **2007**, *91*, 173112.
12. Tsukruk, V. V.; Ko, H.; Peleshanko, S. Nanotube Surface Arrays: Weaving, Bending, and Assembling on Patterned Silicon. *Phys. Rev. Lett.* **2004**, *92*, 065502.
13. Fukuda, T.; Arai, F.; Dong, L. X. Assembly of Nanodevices with Carbon Nanotubes Through Nanorobotic Manipulations. *Proc. IEEE* **2003**, *91*, 1803–1818.
14. Marquardt, C. W.; Blatt, S.; Hennrich, F.; Löhneysen, H.; Krupke, R. Probing Dielectrophoretic Force Fields with Metallic Carbon Nanotubes. *Appl. Phys. Lett.* **2006**, *89*, 183117.
15. Krupke, R.; Hennrich, F.; Löhneysen, H.; Kappes, M. M. Separation of Metallic from Semiconducting Single-Walled Carbon Nanotubes. *Science* **2003**, *301*, 344–347.
16. Chung, J. Y.; Lee, K. H.; Lee, J. H.; Ruoff, R. S. Toward Large-Scale Integration of Carbon Nanotubes. *Langmuir* **2004**, *20*, 3011–3017.
17. Bonard, J.-M.; Stora, T.; Salvetat, J.-P.; Maier, F.; Stöckli, T.; Duschl, C.; Forro, L.; de Heer, W. A.; Châtelain, A. Purification and Size-Selection of Carbon Nanotubes. *Adv. Mater.* **1997**, *9*, 827.
18. Jantoljak, H.; Salvetat, J.-P.; Forro, L.; Thomsen, C. Low-Energy Raman-Active Phonons of Multiwalled Carbon Nanotubes. *Appl. Phys. A: Mater. Sci. Process.* **1998**, *67*, 113–116.
19. HD2200 Bandelin Sonopuls ultrasonic homogenizer probe is dipped into the solution in order to increase the efficiency of the dispersion process. Parameters: 100 W (power 50%), 10 min. The temperature of the sample was kept at 20 °C.
20. Lide, D. R. *CRC Handbook of Chemistry and Physics*, 90th ed. [Online]; CRC Press/Taylor and Francis: Boca Raton, FL, 2010. http://www.hbcpnetbase.com/.
21. Krupke, R.; Hennrich, F; Kappes, M. M.; Löhneysen, H. Surface Conductance Induced Dielectrophoresis of Semiconducting Single-Walled Carbon Nanotubes. *Nano Lett.* **2004**, *4*, 1395–1399.
22. Sanfelix, P. C.; Holloway, S.; Kolasinski, K. W.; Darling, G. R. The Structure of Water on the (0001) Surface of Graphite. *Surf. Sci.* **2003**, *532−535*, 166–172.
23. Walther, J. H.; Jaffe, R.; Halicioglu, T.; Koumoutsakos, P. Carbon Nanotubes in Water: Structural Characteristics and Energetics. *J. Phys. Chem. B* **2001**, *105*, 9980–9987.
24. Zhanpeisov, N. U.; Zhidomirov, G. M.; Fukumura, H. Interaction of a Single Water Molecule with a Single Graphite Layer: An Integrated ONIOM Study. *J. Phys. Chem. C* **2009**, *113*, 6118–6123.
25. Martens, H. C. F.; Reedijk, J. A.; Brom, H. B.; de Leeuw, D. M.; Menon, R. Metallic State in Disordered Quasi-One-Dimensional Conductors. *Phys. Rev. B* **2001**, *63*, 073203.
26. Dimaki, M.; Boggild, P. Dielectrophoresis of Carbon Nanotubes Using Microelectrodes: A Numerical Study. *Nanotechnology* **2004**, *15*, 1095–1102.
27. Battezzati, L.; Pisani, C.; Ricca, F. Equilibrium Conformation and Surface Motion of Hydrocarbon Molecules Physisorbed on Graphite. *J. Chem. Soc., Faraday Trans. 2* **1975**, *71*, 1629–1639.
28. Avgul, N. N.; Kiselev, A. V.; Lygina, I. A. The Adsorption Energies of Water, Alcohols, Ammonia and Methylamine on Graphite. *Russ. Chem. Bull.* **1961**, *8*, 1308–1313.